

## Tunable Plasmonic Crystals for Edge Magnetoplasmons of a Two-Dimensional Electron System

V. M. Muravev,<sup>1,2</sup> A. A. Fortunatov,<sup>2</sup> I. V. Kukushkin,<sup>1,2</sup> J. H. Smet,<sup>1</sup> W. Dietsche,<sup>1</sup> and K. von Klitzing<sup>1</sup>

<sup>1</sup>Max-Planck-Institut für Festkörperforschung, Heisenbergstraße 1, 70569 Stuttgart, Germany

<sup>2</sup>Institute of Solid State Physics, RAS, Chernogolovka, 142432 Russia

(Received 11 March 2008; revised manuscript received 3 September 2008; published 17 November 2008)

Plasmonic crystal effects analogous to photonic crystal phenomena such as zone folding and gap opening were observed for edge magnetoplasmons in a two-dimensional electron system with a periodically corrugated boundary at microwave frequencies. Magnetic field dependent photovoltage data provide unequivocal evidence for Bragg reflection. Band gaps up to fifth order were observed. These gaps were investigated as a function of the electron density, the magnetic field, and the periodicity to demonstrate the tunability of the dispersive properties of these plasmonic crystals.

DOI: 10.1103/PhysRevLett.101.216801

PACS numbers: 73.20.Mf, 71.36.+c

Photonic crystals, composed of spatially periodic dielectric structures, have attracted considerable attention as they offer control over electromagnetic waves at the wavelength level. They influence wave propagation, typically in the visible or near-infrared part of the spectrum, in a similar manner as the periodic potential in a crystal affects the electron motion. Through Bragg reflection, allowed and forbidden energy bands are defined. The photonic gaps, which may be present, as well as the dispersion and refraction properties of these periodic structures give rise to potentially useful optical phenomena such as the inhibition of spontaneous emission, low-loss wave-guiding, and negative refraction [1]. If the wave is incident on a conducting, usually metallic, surface, the presence of free electrons gives rise to a resonant interaction between collective surface charge oscillations and the electromagnetic field and so-called surface plasmon polaritons form [2,3]. They propagate along the surface and possess a more complex dispersion than the linear dispersion of light. Periodic texturing of the conducting surface modifies this dispersion through zone folding and gap opening as in a photonic dielectric crystal [4,5]. The dispersive properties of such a plasmonic crystal as well as of photonic crystals are determined by the geometrical parameters and the chosen materials. Hence, they are normally fixed once the crystal has been fabricated.

In a two-dimensional electron system (2DES), the electron confinement restricts the propagation of plasmon modes to a plane as well and hence similar physics as at metal surfaces is bound to occur [6–8]. The general properties of these classical waves in the 2DES were reviewed in Ref. [9]. Early attempts to observe Bragg reflection of plasmons in the 2DES were carried out on Silicon MOSFETs with a patterned top gate to periodically modulate the density [10–12]. These experiments were hampered by plasma decay over short distances. Since then the quality of 2DESs has improved dramatically and plasmons can propagate over millimeter distances in GaAs 2D systems [13]. Compared with photonic crystals and patterned metallic surfaces, the 2DES offers powerful addi-

tional degrees of freedom to alter the dispersive properties of the plasmonic crystal after its fabrication, since the properties of plasmons can be tuned through the application of a perpendicular magnetic field  $B$  or by changing the electron density  $n_s$  with the field effect. While the  $n_s$  and  $B$  both influence the plasmon velocity, the application of a  $B$ -field also affects the spatial width of the excitations. The dimensionality of some of the plasma excitations changes. Edge magnetoplasma waves [14–17] of one-dimensional character emerge. An “omnidirectional” photonic band gap then only requires a periodic variation of some sample property in a single dimension, the remaining propagation direction. Here, we have investigated whether it is possible to observe gaps in the spectrum of edge magnetoplasmons in a plasmonic crystal consisting of a stripe of a 2DES whose width has been varied periodically. “Plasmonic” gaps up to fifth order were observed. We demonstrate that their center frequency can be controlled by  $B$  and  $n_s$ .

These studies were carried out on a GaAs-Al<sub>0.3</sub>Ga<sub>0.7</sub>As 2DES. Samples were patterned into mesa geometries as depicted in Fig. 1. That mesa consists of a central rectangular body with a source and drain contact at each end. A total of six legs, which also terminate in an alloyed contact, protrude from the main body. Opposite legs are identical in shape. One leg has a simple rectangular shape, while for the others the width is periodically varied. They will be referred to as plasmonic crystals of period  $p$ . The dimensions in microns are shown in Fig. 1. The density and mobility of the two-dimensional electron system were  $n_s = 1.4 \times 10^{11} \text{ cm}^{-2}$  and  $\mu = 10^6 \text{ cm}^2/\text{V s}$ . It was possible to tune the density up to  $n_s = 3.2 \times 10^{11} \text{ cm}^{-2}$  via the persistent photoconductivity effect by illuminating the sample briefly with red light. The device was placed near the end of a rectangular metallic waveguide (16 mm  $\times$  8 mm) in order to illuminate it with microwaves with frequencies between 40 and 150 GHz and power levels ranging from 10 to 0.1 mW. Sample and waveguide were immersed in liquid helium in a cryostat with a superconducting magnet. The amplitude of the microwave radiation was modulated at 1 kHz. The microwave induced photo-

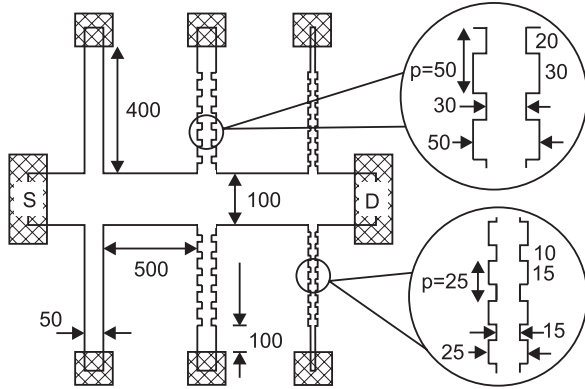


FIG. 1. The device consists of a rectangular mesa from which six legs protrude. Legs either are simple rectangles or exhibit a periodically varying width. The legs with spatially varying width are referred to as plasmonic crystals. Their periodicity  $p$  is either 25 or 50  $\mu\text{m}$ . All dimensions are in microns.

voltage, which developed between the drain ( $D$ ) or source ( $S$ ) contact and one of the contact legs ( $C$ ), was detected with a lock-in amplifier at 4.2 K as a function of the applied  $B$  field.

The outcome of such an experiment is illustrated in Fig. 2(a). It shows the photovoltage as a function of  $B$  for two geometrical configurations. The middle curve presents data recorded between the source contact and the leg with constant width, while the top curve is for a leg with a periodically varying width ( $p = 50 \mu\text{m}$ ). The stripe of constant width produces rapid, approximately  $B$ -periodic oscillations. These oscillations were observed previously [13,18–20]. They were attributed to the coherent propagation of edge magnetoplasmons, which emerge in the presence of a perpendicular field. The following scenario was envisaged. The microwave radiation couples to the metallic contact and triggers edge magnetoplasmons in the 2DES with electric and magnetic fields oriented as drawn in the inset to Fig. 2(a). A theoretical treatment of the excitation of plasmon polaritons in a 2DES with an embedded contact was recently reported in Ref. [21]. The metallic contact mediates momentum transfer, so the radiation can couple to excitations with nonzero momenta. Hence, the metallic contact serves a similar role as gratings in metallic systems or the 2DES [8]. The edge magnetoplasmons are chiral in nature and are forced to propagate along the boundary in a direction dictated by the sign of  $B$ . Experiments on the leg without a boundary corrugation have shown that an abrupt change in the geometry, i.e., the sample width, at the end of the leg causes scattering and reflection of the edge magnetoplasmon, which moves upward and comes from the metallic contact (lower inset in Fig. 2(a)). At least part of the wave is converted into the edge magnetoplasmon which propagates in the opposite direction back to the metallic contact on the other side of the leg, provided the width of the leg is sufficiently small. The injected and reflected waves interfere near the metallic contact. For constructive interference, the large ac signal

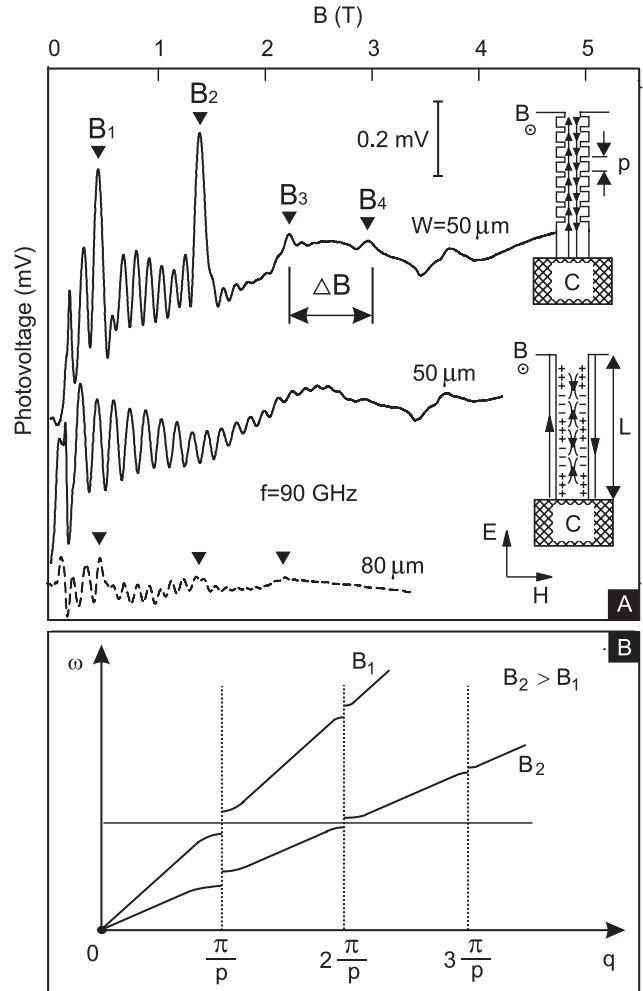


FIG. 2. (a)  $B$ -field dependence of the photovoltage measured across the source contact and either the contact of the leg with constant width (middle trace) or the leg with a corrugated boundary with period  $p = 50 \mu\text{m}$  (upper trace). The upper curve exhibits large amplitude and less frequent  $B$ -periodic features, marked as  $B_i$  with  $i = 1, 2, \dots$ . They are attributed to Bragg reflection of edge magnetoplasmons. The distance between adjacent Bragg peaks is denoted as  $\Delta B$ . The data were recorded for  $n_s = 3.2 \times 10^{11} \text{cm}^{-2}$ . The bottom dashed curve displays the photovoltage for an 80  $\mu\text{m}$  wide corrugated leg. The significant reduction of the Bragg peaks results from a decreased coupling between upward and downward moving waves for this wider plasmonic crystal. (b) Schematic illustration of how the edge magnetoplasmon dispersion is modified in a geometry with a corrugated boundary. For simplicity a linear dispersion has been assumed. Gaps appear at the Brillouin zone boundaries defined by the periodicity  $p$ . As  $B$  is tuned, the dispersion changes and the gaps shift to different frequency intervals.

may cause rectification and a dc photovoltage develops [18]. Rectification may arise from the nonideal characteristic of the Ohmic contact or as a result of different boundary conditions at either end of the propagation path of the plasmon wave as described in the context of short channel ballistic field effect transistors in Ref. [22]. Sufficiently far away from  $B = 0$ , the plasmon branch,

whose frequency drops with increasing  $B$ , may be regarded as a magnetoplasmon confined to the edge. A simple linear dispersion provides a good approximation [17] (a logarithmic term is discarded as it only changes weakly):

$$\omega \propto n_s q / B. \quad (1)$$

Here,  $\omega$  is the frequency of the incident radiation and the edge magnetoplasmon. For interference to occur,  $q$  should take on an integer multiple of  $\pi/L$ , where  $L$  is the total length of the leg. At fixed density and incident radiation frequency, a  $B$ -periodic oscillatory photovoltage is expected with period  $\Delta B \propto n_s / (L\omega)$ . These dependencies are indeed born out in experiment.

For the leg with a periodically varying width, coupling of the injected upward moving edge magnetoplasmon with its downward moving counterpart is promoted near each constriction and it may be anticipated that the corrugated leg boundary acts as a plasmonic Bragg reflector. Peaks in the photovoltage should arise when the Bragg rule  $q = (\pi/p)N$ , with  $N$  is an integer, is fulfilled and all the reflected waves from each unit cell constructively interfere. When combining the Bragg rule with the plasmon dispersion described by Eq. (1), Bragg reflection should produce  $B$ -periodic oscillations with a period

$$\Delta B \propto n_s / (\omega p), \quad (2)$$

for fixed  $\omega$ . These Bragg peaks coincide with gaps in the energy dispersion of increasing order, as illustrated in Fig. 2(b). The larger amplitude and less frequent peaks in the top trace of Fig. 2(a), which have been denoted as  $B_1$  through  $B_4$ , are assigned to the fundamental and up to fourth order gaps introduced by the plasmonic crystal in the dispersion. These data were recorded for a leg with  $W = 50 \mu\text{m}$ . The amplitude of the Bragg peaks drops significantly for larger values of  $W$  due to the decreased coupling in wider crystals between upward and downward moving waves. This damping of the Bragg features is illustrated in the bottom trace of Fig. 2(a) ( $W = 80 \mu\text{m}$ ). In the remainder, we will corroborate this picture by altering all parameters in Eq. (2): the frequency  $\omega$ , the density  $n_s$  and the period  $p$ . Note that the observation of these features implies coherent propagation of plasmons over millimeter distances, magnitudes larger than the coherence length of electrons at these temperatures.

Figure 3 illustrates the influence of the microwave frequency on the  $B$ -dependent photovoltage. The data were recorded on a plasmonic crystal with a period  $p = 50 \mu\text{m}$ . The Bragg peaks shift and the periodicity  $\Delta B$  of the oscillations decreases with increasing microwave frequency in accordance with Eq. (2). The inset plots the  $B$  values at which Bragg reflection occurs as a function of the microwave frequency. The Bragg peaks shift continuously even down to small field values where plasmons are no longer confined close to the edge. The solid lines are the result of a theoretical simulation which goes beyond Eq. (1) to properly describe the plasmon dispersion also at

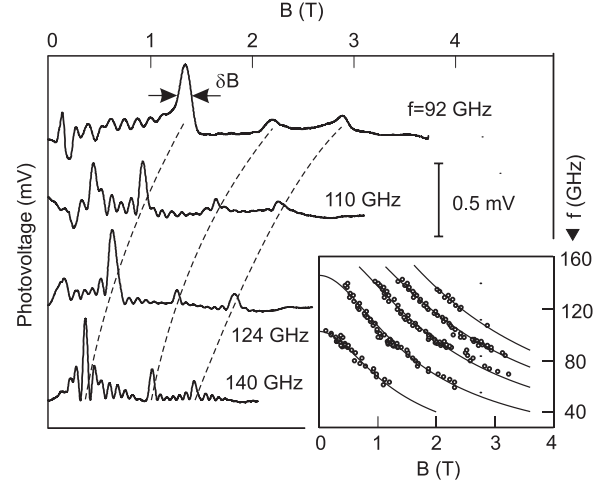


FIG. 3. The photovoltage versus  $B$  in a plasmonic crystal with period  $p = 50 \mu\text{m}$  and  $\omega$  as a parameter. The period of the Bragg features decreases with increasing  $\omega$ . The inset plots the  $B$  values where Bragg reflection occurs for many frequencies. These results are compared with theoretical simulations based on the dispersion of edge magnetoplasmons as derived in Ref. [23]. The data were recorded for  $n_s = 3.2 \times 10^{11} \text{ cm}^{-2}$ .

smaller fields. The edge magnetoplasmon branches may be described by the following functional form [23,24]:

$$\omega_{\text{EMP}}(B) = \omega_i / \sqrt{1 + (B/B_0)^2}. \quad (3)$$

Here,  $\omega_i$  is the zero field frequency of the fundamental ( $i = 1$ ) and higher order modes ( $i = 2, 3, \dots$ ). It can be estimated numerically from the geometry of the unit cell of the plasmonic crystal. Here, it has served as a fit parameter. The field  $B_0$  has also been taken as a fit parameter, but was chosen identical for all simulation curves, i.e., independent of the index  $i$ .

The width  $\delta B_i$  of the photovoltage peak at field  $B_i$  associated with Bragg reflection can in conjunction with the data in the inset of Fig. 3 be used to estimate the size of the  $i$ th "plasmonic" gap in the plasmon dispersion. The gap size will be referred to as  $\delta\omega_i$  and can be rewritten as  $(\partial\omega_i/\partial B)\delta B_i$ , where  $\partial\omega_i/\partial B$  is the slope of the curves in the inset to Fig. 3. For 82 GHz, the following gap sizes are obtained:  $\delta\omega_1/2\pi = 3.6 \text{ GHz}$ ,  $\delta\omega_2/2\pi = 3.3 \text{ GHz}$ ,  $\delta\omega_3/2\pi = 3.1 \text{ GHz}$ , and  $\delta\omega_4/2\pi = 2.9 \text{ GHz}$ . The accuracy with which we can determine these gap widths from the experimental data depends on the order. For well pronounced peaks it is approximately 10%. We conclude that the band gaps only weakly depend on the index; i.e., the amplitude of the Fourier components determining the scattering potential only drops weakly for higher order. It suggests that scattering of the edge magnetoplasmon waves is strongly localized in space, presumably at the corner between two regions of different width. The plasmon wavelength is much larger than the radius of the lithographically defined corner. Additional experiments have shown that the number of periods of the Bragg

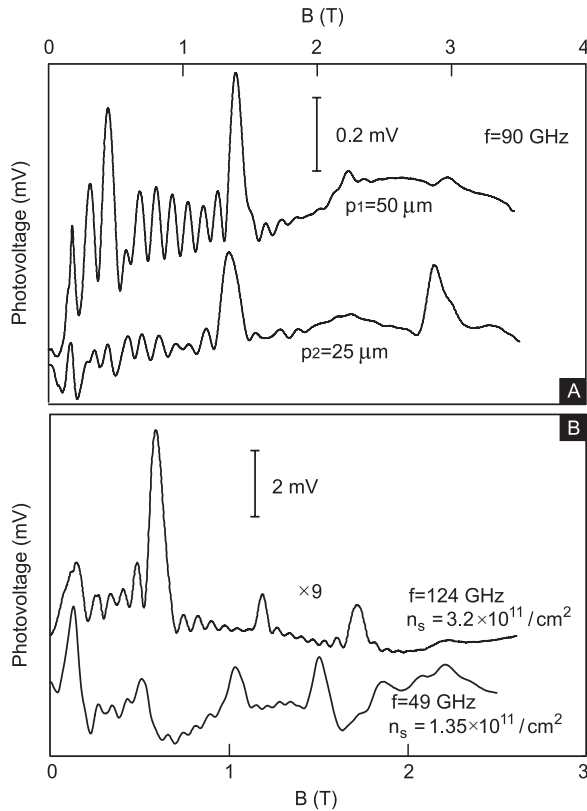


FIG. 4. (a) Influence of the plasmonic crystal period on the photovoltage Bragg oscillation period. A doubling of  $p$  halves  $\Delta B$ . (b)  $B$  dependence of the photovoltage in a plasmonic crystal with  $p = 50 \mu\text{m}$  for two densities. To keep the period of the Bragg peaks constant, the microwave frequency has been scaled by approximately the ratio of the densities.

reflector plays an important role. However, an increase of this number beyond ten has no significant effect on the peak width, because the plasma damping length becomes smaller than the length of the Bragg structure.

Figure 4 shows how the period  $p$  of the plasmonic crystal (panel A) and the density  $n_s$  (panel B) affect  $\Delta B$ . If the period doubles, the distance between the Bragg peaks halves. This agrees well with Eq. (2) and reflects the larger energy separation between adjacent gaps as the period  $p$  shrinks [Fig. 2(b)]. These data also exclude that the observed peaks are a result of a single reflection off the very first interface as the distance between the metallic contact and the first interface remains fixed. Panel B illustrates that the period  $\Delta B$  remains essentially constant when  $n_s$  and  $\omega$  are simultaneously scaled by the same factor. For panel B the ratio of the frequencies and the density for the two data traces are both approximately equal to 2.4. These measurements are a vivid illustration of the additional degrees of freedom the 2DES offers over other photonic dielectric or metallodielectric crystals for fabricating plasmonic crystals. The dispersive properties can be tuned *in situ*.

In conclusion, we have investigated the propagation of edge magnetoplasmon waves in a plasmonic crystal con-

sisting of a stripe of a two-dimensional electron system whose width varies in a periodic manner. The fundamental as well as higher order gaps, which appear in the spectrum of the edge magnetoplasmons as a result of zone folding and Bragg reflection have been detected. The frequency of these gaps were studied as a function of the electron density, the applied magnetic field and the period of the plasmonic crystal. We anticipate that also periodic modulations of the density or other parameters influence the plasmon properties and would produce similar results.

We acknowledge financial support from the Russian Foundation for Basic Research (RFBR), INTAS, the DFG and the BMBF. V.M.M. is grateful for financial support from the Forschungszentrum Jülich.

- 
- [1] J.M. Lourtioz *et al.*, *Photonic Crystals* (Springer, New York, 2005).
  - [2] E. Ozbay, *Science* **311**, 189 (2006).
  - [3] W.L. Barnes, A. Dereux, and T.W. Ebbesen, *Nature* (London) **424**, 824 (2003).
  - [4] S.C. Kitson, W.L. Barnes, and J.R. Sambles, *Phys. Rev. Lett.* **77**, 2670 (1996).
  - [5] S.I. Bozhevolnyi, J. Erland, K. Leosson, M.W. Skovgaard, and J.M. Hvam, *Phys. Rev. Lett.* **86**, 3008 (2001).
  - [6] F. Stern, *Phys. Rev. Lett.* **18**, 546 (1967).
  - [7] C.C. Grimes and G. Adams, *Phys. Rev. Lett.* **36**, 145 (1976).
  - [8] S.J. Allen, D.C. Tsui, and R.A. Logan, *Phys. Rev. Lett.* **38**, 980 (1977).
  - [9] V.A. Volkov and S.A. Mikhailov, in *Modern Physics in Condensed Matter Sciences*, Landau Level Spectroscopy Vol. 27.1, edited by G. Landwehr and E.I. Rashba (North Holland, Amsterdam, 1991), p. 855.
  - [10] U. Mackens *et al.*, *Phys. Rev. Lett.* **53**, 1485 (1984).
  - [11] R.J. Wilkinson *et al.*, *J. Appl. Phys.* **71**, 6049 (1992).
  - [12] M.V. Krasheninnikov and A.V. Chaplik, *Fiz. Tekh. Poluprovodn.* **15**, 32 (1981).
  - [13] V.M. Muravev *et al.*, *JETP Lett.* **83**, 246 (2006).
  - [14] S.J. Allen, Jr., H.L. Störmer, and J.C.M. Hwang, *Phys. Rev. B* **28**, 4875 (1983).
  - [15] D.B. Mast, A.J. Dahm, and A.L. Fetter, *Phys. Rev. Lett.* **54**, 1706 (1985).
  - [16] D.C. Glatli *et al.*, *Phys. Rev. Lett.* **54**, 1710 (1985).
  - [17] V.A. Volkov and S.A. Mikhailov, *Zh. Eksp. Teor. Fiz.* **94**, 217 (1988) [*Sov. Phys. JETP* **67**, 1639 (1988)].
  - [18] I.V. Kukushkin *et al.*, *Phys. Rev. Lett.* **92**, 236803 (2004).
  - [19] I.V. Kukushkin, S.A. Mikhailov, J.H. Smet, and K. von Klitzing, *Appl. Phys. Lett.* **86**, 044101 (2005).
  - [20] B. Simović *et al.*, *Phys. Rev. B* **71**, 233303 (2005).
  - [21] A. Satou and S.A. Mikhailov, *Phys. Rev. B* **75**, 045328 (2007).
  - [22] M. Dyakonov and M. Shur, *IEEE Trans. Electron Devices* **43**, 380 (1996).
  - [23] I.L. Aleiner, D. Yue, and L.I. Glazman, *Phys. Rev. B* **51**, 13467 (1995).
  - [24] I.V. Kukushkin *et al.*, *Phys. Rev. B* **72**, 161317 (2005).